Case Studies in Thermal Engineering 37 (2022) 102259

Contents lists available at ScienceDirect

Case Studies in Thermal Engineering

journal homepage: www.elsevier.com/locate/csite

Spray characteristics of fouled gasoline direct injectors under flash boiling and sub-zero temperature conditions

Donghwan Kim [a], Sungwook Park [b,*]

[a] Department of Mechanical Convergence Engineering, Graduate School of Hanyang University, Seoul, 04763, Republic of Korea
[b] School of Mechanical Engineering, Hanyang University, Seoul, 04763, Republic of Korea

ARTICLE INFO

Keywords:
Gasoline direct injector
Flash boiling
Fouled injector
Mie-scattering
Spray visualization
High-speed imaging

ABSTRACT

This study investigated the spray characteristics of a fouled injector under different ambient pressures, fuel temperatures, and flashing ratios. Four fouled injectors and a clean injector were used to analyze the effects of deposits on spray characteristics. A fouled injector, showing the greatest difference in spray characteristics compared to a clean injector, was selected as a representative fouled injector and analyzed. The near-field and far-field spray visualization were performed by using the Mie-scattering imaging technique. Quantitative indices, such as the spray angle, penetration length, and sharpness intensity, were defined to compare the spray characteristics of the fouled and clean injectors. These quantitative indices were calculated using the MATLAB image processing tool. Deposits formed differently even under the same engine operating condition, such that the spray structure was different depending on the fouled injector. In the near-field spray visualization, there were relatively large droplets and long ligaments in the fouled injector compared to the clean injector due to the low atomization performance.

1. Introduction

Gasoline direct injection (GDI) engines are widely used worldwide due to the advantages of high engine efficiency, low fuel consumption and exhaust gases, and the possibility of using different clean alternative fuels [1–3]. In a GDI engine, the fuel injector is installed inside the combustion chamber and fuel is supplied directly into the combustion chamber. The result of this process is that there is a shorter time to form an ideal mixture formation compared to the port fuel injection (PFI) method [4]. Therefore, by applying a relatively high injection pressure, the atomization performance is improved, and the air-fuel mixture is efficiently mixed in a short time. Due to the high injection pressure, the spray penetration length is relatively long, which increases the possibility of wall-wetting, such as wetting of the cylinder wall and piston head [5,6]. Therefore, in GDI engines, the selection of the spray pattern and the injection strategy depending on the combustion mode play an important role in the engine performance. In many studies, various types of injectors have been designed and applied, such as side-mounted injection and center-mounted injection, to increase the efficiency of GDI engines [7,8]. Because the GDI engine exposes the injector to high-temperature and high-pressure conditions inside the combustion chamber, many factors in normal engine operating conditions cause deposits on the injector [9,10]. Deposits can occur inside and outside the injector nozzle, resulting in a reduced fuel mass flow rate, unexpected spray patterns, and low atomization performance [11,12]. A decrease in the atomization performance and the occurrence of wall-wetting by an excessive increase of spray penetration length can directly affect soot generation. Therefore, many previous studies have researched the effect of deposits on spray

* Corresponding author. School of Mechanical Engineering, Hanyang University, 222 Wangsimni-ro, Seongdong-gu, Seoul, 04763, Republic of Korea.
E-mail address: parks@hanyang.ac.kr (S. Park).

https://doi.org/10.1016/j.csite.2022.102259
Received 5 May 2022; Received in revised form 27 June 2022; Accepted 1 July 2022
Available online 5 July 2022
2214-157X/© 2022 The Authors. Published by Elsevier Ltd. This is an open access article under the CC BY-NC-ND license (http://creativecommons.org/licenses/by-nc-nd/4.0/).

characteristics to solve these problems.

Bo et al. investigated the effects of deposits on spray characteristics with experiments [13]. Moreover, the mixture formation at 1200 rpm and injection pressure of 150 bar was studied by simulation based on the experimental results. They found that deposits caused a decrease in the injection quantity, and produced a long spray penetration length. Higher droplet velocities and larger droplet sizes were caused by the smaller effective nozzle cross-sectional area and clogging deposits in the counterbore. Furthermore, injector deposits led to more fuel impingement on the piston and cylinder wall and distortion of the spray pattern. Therefore, with deposits, an unideal mixture formation occurred that was demonstrated by unstable engine performance. Jianwei et al. investigated the near-nozzle spray development of a typical fouled GDI injector [14]. They found that deposit could be the main reasons for increased soot emissions, because the interaction between deposits and spray led to several poor spray behaviors, such as spray distortion, residual fuel stored in the nozzles and deposits layer, along with liquid splashing, ligaments and large droplets, and tip wetting or dripping. Due to the low atomization performance of the fouled injector, a relatively high quantity of droplets and ligaments were observed even as the injection pressure increased. From these results, they found that high injection pressure did not improve the atomization performance in a fouled injector. Moreover, droplets remained and were suspended around the injector tip. Some droplets

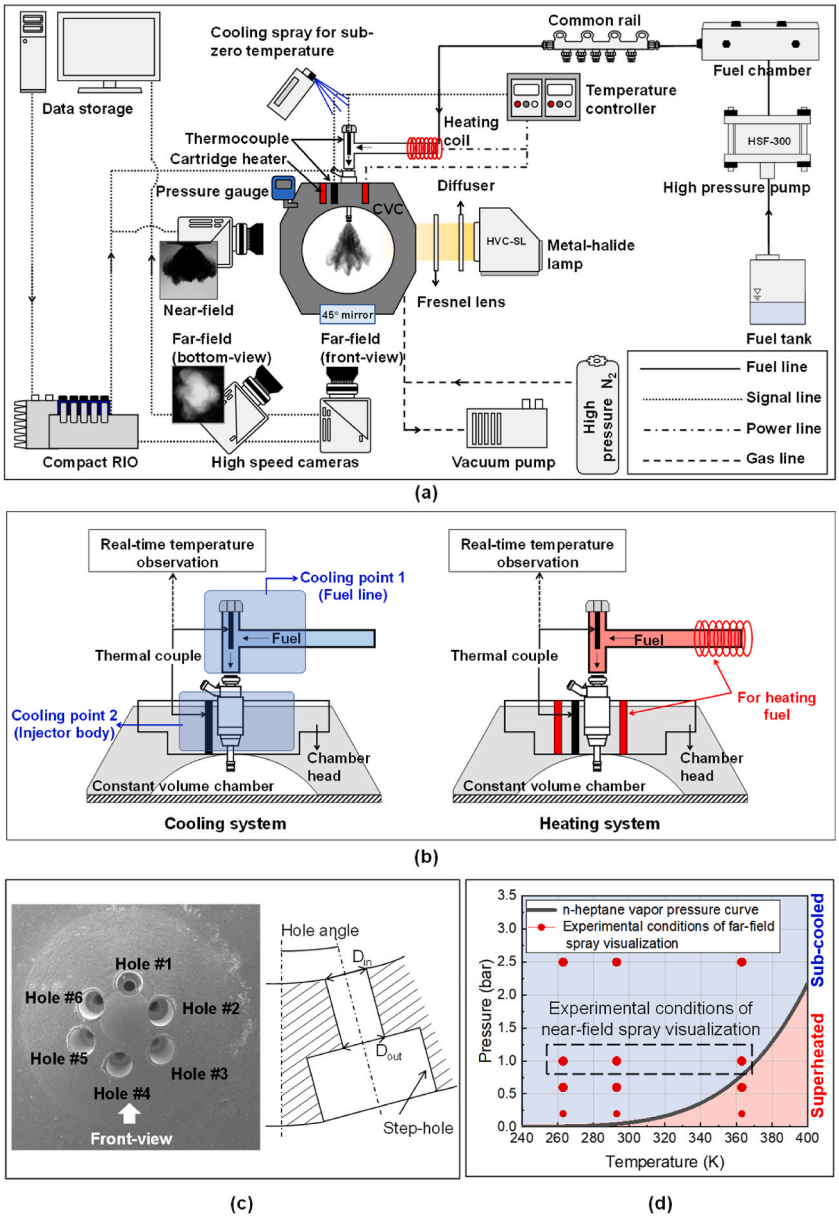

Fig. 1. Experimental information: (a) schematic of the spray visualization system, (b) detailed schematic of the cooling and heating system, (c) nozzle geometry, and (d) experimental conditions of the spray visualization with the vapor pressure curve of the test fuel.

moved back to the injector tip and caused tip wetting. Deposits are affected directly by the surface of the nozzle tip, so Zhou et al. investigated the effects of surface temperature on the deposit behaviors of gasoline on a hot surface [15]. The surface temperature of the nozzle tip significantly affected the evaporation of gasoline droplets. The form of the deposit affected the evaporation of the gasoline. The variation of deposit quantities with the increase of temperature presented two peaks. Moreover, the morphology and components of deposits at each peak were completely different, indicating a difference in the reactants and reaction path at different temperatures.

From the previous research, various spray characteristics can be observed in fouled injectors because deposits can be formed in various shapes even under the same engine operating conditions. Therefore, the results of previous studies cannot represent the spray characteristics of the fouled injector. In addition, spray characteristics vary greatly depending on injection conditions. However, studies about effects of deposits on spray characteristics depending on injection conditions are still lacking. In fact, fuel can be injected into the engine under various conditions such as high-temperature, high-pressure, low-temperature, low-pressure, and flash-boiling conditions, and the spray characteristics vary greatly in these various injection conditions.

In the design of the injector, various factors such as spray pattern, spray angle, and spray structure are considered to optimize fuel supply into the combustion chamber. However, injector deposits can be generated by various reasons, so that unexpected spray results can be shown. Therefore, in this study, effects of deposits on the spray characteristics under various injection conditions including flash boiling and low-temperature conditions were investigated. At first, the spray characteristics in the four fouled injectors were analyzed under the same engine operating condition. Among them, the most fouled injector, showing the greatest difference from the clean injector, was selected as the representative fouled injector. The deposit images were captured by Scanning Electron Microscopy (SEM) equipment. After that, the interaction between plumes, atomization performance, and the residual droplets at the end of injection were compared through near-field spray visualization under atmospheric pressure conditions. Moreover, the spray characteristics of the fouled injector were analyzed depending on ambient pressure, fuel temperature, and flash boiling occurrence through far-field spray visualization.

2. Experimental setup

Mie-scattering and diffuse back-illumination (DBI) methods were employed in the two spray experiments: near-field and far-field spray visualizations. The schematic of the spray visualization is drawn in Fig. 1(a). A fuel pump and chamber were used to realize the various injection pressure conditions. A common rail was used to reduce the pressure fluctuation and pulsation. Test injectors were controlled by using a Compact RIO (NI, USA) controller. A metal-halide lamp was used as a light source and the time-dependent spray images were captured by a high-speed camera (VEO 1310, Phantom). In this study, DBI imaging technique was applied to analyze the spray characteristics in near-field spray visualization. The possibility of saturation of scattered light could be decreased by using DBI imaging technique. Therefore, behavior of droplets and ligaments can be analyzed clearly. We used Mie-scattering imaging technique for simultaneous experiment of spray visualization in bottom-view and in front-view using two high-speed cameras. The details concerning the camera setup are tabulated in Table 1. A constant volume chamber (CVC) with an inner diameter of 200 mm, a vacuum pump, and nitrogen gas were used to realize the various ambient pressures. The head of the CVC was heated by two cartridge heaters with a K-type thermocouple. The heaters were located as close as possible to the test injector. Moreover, a section of 300 mm from the injector was heated by a heating coil to increase the fuel temperature. Sub-zero temperature conditions were realized by using a cooling spray. In this study, to maintain and confirm the fuel temperature, temperature sensors were located at the CVC head and fuel line. Therefore, the exact temperature conditions could be realized. The fuel temperature inside the nozzle is an important factor which should be controlled during the experiment. However, there was limitation of measuring fuel temperature inside nozzle tip in the heating and cooling system. Therefore, in this study, we assumed that the fuel temperature was the same as the surface of the injector body temperature. To maintain the temperature of injector body, heating and cooling system was composed as Fig. 1(b). The temperature of the fuel supplied into the injector was measured by a thermocouple installed in the fuel line. During the experiment, the temperature was observed in real-time, and continuous cooling or heating were performed. Therefore, the temperature of the fuel could be maintained. Moreover, a thermocouple was installed as close as possible to the injector body. The temperature near injector body was also observed in real-time. The cooling spray was sprayed continuously to maintain the injector body temperature during the low-temperature experiment. The test injectors had a small injection quantity per shot. And only fuel injection of 10 times were performed. Therefore, we could maintain the temperature of injector body during the experiment.

Fig. 1(c) shows an SEM image with a low magnification of the clean injector. The number of holes was six, and the hole angle was from a minimum of 3.05 ° to a maximum of 33.52 °. The type of test injector was a side-mounted solenoid type. The specifications of the test injector are listed in Table 2.

Table 1
The spray visualization setup parameters.

Items	Details	
	Near-field	Far-field
Exposure time (μs)	0.68	10
Resolution (pixels)	960 × 960	600 × 800 (Front-view) 600 × 832 (Bottom-view)
Frame rate (fps)	10,000	

2.1. Experimental parameters

Near-field and far-field spray visualizations were conducted by using Mie scattering and DBI imaging techniques to observe the difference of spray characteristics in fouled and clean injectors. The spray visualization using four fouled injectors and a clean injector was conducted to confirm the effects of deposits on spray characteristics and to study the shot-to-shot variation. Near-field spray visualizations of a representative fouled injector and clean injector were conducted to understand the spray atomization performance, plume-to-plume interaction, and the spray characteristics at the end of injection. The far-field spray visualizations using a fouled and clean injector were conducted using a front-view and bottom-view under various ambient and fuel temperature conditions, including flash boiling conditions. This visualization was conducted to analyze the effects of deposits on spray characteristics under flash boiling and sub-zero temperature conditions. The details about the experimental conditions are tabulated in Table 3.

The nozzle temperature varied from 266 to 363 K. The selected ambient pressures were 0.2, 0.6, 1.0, and 2.5 bar. In the experimental conditions, the superheated conditions are displayed in Fig. 1(d).

2.2. Spray image post-processing procedure and definitions of quantitative indices

Spray images were processed by MATLAB (MathWorks, USA) in the order shown in Fig. 2. The number of black pixels were calculated by process in Fig. 2(a) to analyze quantitatively the results of near-field spray images. The original image was cropped by excluding out-of-focus areas. The nozzle tip was eliminated after original image was cropped. Finally, the deleted nozzle image was binarized to count the number of black pixels. In this study, the spray visualization experiment was repeated 10 times with an injection frequency of 1.67 Hz. The thresholding value was defined as 5% of the highest intensity of each spray image to convert from the deleted background grayscale image, as shown in Fig. 2(a) to produce the binarized image. The spray boundary was detected based on the binarized image. In the far-field spray visualization, the spray angle and penetration length were calculated by detecting the spray boundary. The penetration length was defined as the longest distance from the injector nozzle tip. The spray angle was measured at the upper end of the spray where the effect of drag is relatively small because the lower end of the spray is greatly affected by the drag force. Therefore, the spray angle was calculated within 1/3 of the penetration length. Moreover, sharpness intensity was defined to compare the sharpness of the spray structure in the bottom-view. The plume-to-plume interaction was compared by using the sharpness intensity which is a quantitative index in the fouled and clean injectors. The process of calculating the sharpness intensity is depicted in Fig. 2(b). The original spray images of the 10 injections are superposed to derive the average spray structure. The superposed image was converted as a binarized image, and the centroid of spray was measured. A circle having the same area as the spray area was drawn based on the centroid. The area outside the circle was calculated, and the ratio of the circle area (Area 1) and area outside the circle (Area 2) was defined as the sharpness intensity (Area 2/Area 1). A sharpness intensity close to 0 means that the shape of the bottom-view is closer to a circle and there is more interaction between the plumes.

3. Results and discussion

3.1. Comparison of spray characteristics in four fouled injectors

It is hard to define the effects of deposits on the spray characteristics because various formations of deposits can be produced even under the same engine operating conditions. Therefore, in this study, the spray characteristics of four fouled injectors with deposits that occurred under the same engine operating conditions were compared. Immediately after the formation of the deposits, the deposits that were weakly attached might be washed off by the initial fuel injection. Moreover, the injection order might affect the spray structure. Therefore, the penetration lengths depending on the injection order were also analyzed in the four fouled injectors.

The spray structures and shot-to-shot variations of the four fouled injectors are depicted in Fig. 3(a). The spray structure was different depending on injectors due to the different deposit formations, even though the fouled injectors had the same nozzle configuration, and the deposits were formed under same engine operating condition in 4-cylinder GDI engine. The sharpest spray structure that had clear distinguished plumes is observed for fouled injector 1. Moreover, the variation of the penetration length was the highest in fouled injector 1, as shown in Fig. 3(b). The standard deviations of the penetration lengths depending on time were lower than 4 mm in the fouled injectors, except for the fouled injector 1. However, in all fouled injectors, the injection order did not have significant effects on the spray structure and showed different random spray structures from the 1st to 10th injection. In the case of fouled injector 1, the shot-to-shot variation increased steeply after a TASOE of 0.8 ms. This is because the variation of injection quantity and atomization performance by deposits affected the penetration length. In the case of the other injectors, a relatively similar level of shot-to-shot variation was observed. The average penetration lengths with standard deviations of the four fouled injectors are compared in Fig. 3(c). The sharpest plumes were observed in the case of the fouled injector 1. During the spray development, the

Table 2
Specifications of the test injectors.

Items	Details
Number of holes	6
Hole angle (°)	Min. 3.05, Max. 33.52
D_{in}/D_{out}	1.15
Flow rate per a hole (cc/min)	70
Hole diameter (μ m)	150
Type	Solenoid, side mount and sac type injector

Table 3
Test conditions.

Items	Details		
Test injectors	Four fouled injectors, clean injector	Representative fouled injector, clean injector	
Visualization area	Far-field (Front-view)	Near field (Front-view)	Far-field (Front and bottom-view)
Nozzle temperature (K)	293	266, 293, 363	
Ambient pressure (bar)	1.0		0.2, 0.6, 1.0, 2.5
Test fuel	n-heptane		
Energizing duration (ms)	2.0		
Injection pressure (bar)	100, 200		

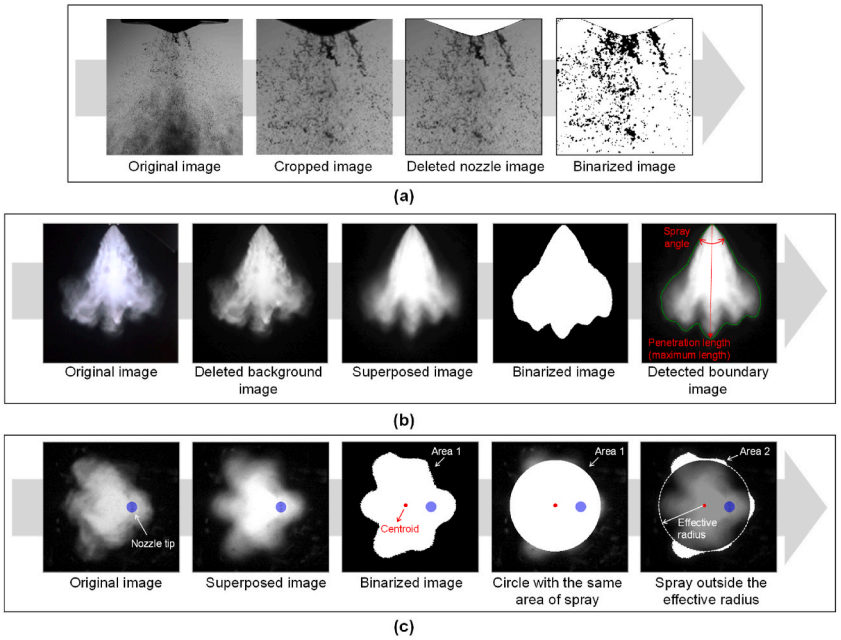

Fig. 2. Image processing: (a) process of calculating number of black pixels in near-field spray visualization, (b) process of calculating penetration length and spray angle, and (c) process of calculating spray sharpness.

average of the penetration length was the longest in the injector 1. This is because the atomization performance was lowest in injector 1, so the relatively large droplets could have resistance to the drag force [16]. Even under the same engine operating conditions, deposits can occur in different forms and affect the spray characteristics. Therefore, deposit injectors selected as representative fouled injector in this study cannot represent all fouled injectors. However, we focused on predicting effects of deposits on engine performance. Therefore, by selecting the fouled injector, which shows the greatest difference compared to the clean injector, as the representative fouled injector, it is possible to discuss the effect of the spray characteristics of deposit more clearly. Therefore, the fouled injector 1 was selected as a representative fouled injector because it had the sharpest plumes and longest penetration lengths compared to the clean injector and the other fouled injectors.

3.2. Comparison of deposit formation of holes, injection quantity and rate in the fouled and clean injector

Fig. 4(a) presents the SEM pictures of clean and fouled injectors. The injector tip was covered with a thick layer of deposits. The surface of the hole was rough due to the deposits. The formation of deposits was different for every nozzle hole. However, the stepped holes were clogged, such that the nozzle outlet area was decreased in all holes. The injection quantity and rate are shown in Fig. 4(b). The injection quantity of the clean injector was higher compared to the injection quantity of the fouled injector (minimum 1.2%, maximum 3.8%). The mass flow rate also decreased in the fouled injector. However, there was no difference in the injection delay or nozzle closing delay. It is considered that this is because deposits did not occur enough to affect the injector needle motion. The comparison of standard deviation of penetration length in fouled and clean injectors was also shown in Fig. 4(b). There was relatively large standard deviation of penetration length in fouled injector from 1st to 10th injection. However, the standard deviations of penetration lengths were shown as a similar level in fouled and clean injectors after fuel injection of 50 times. Additional experiments such as near-field and far-field spray visualizations under various injection conditions were performed after acquiring repeatability of the test.

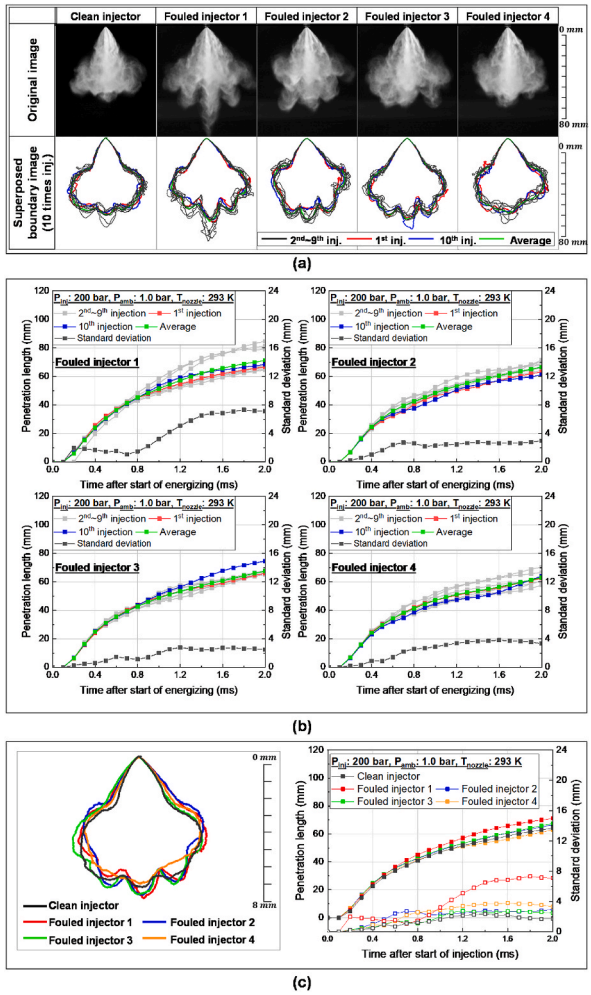

Fig. 3. Spray structures and penetration lengths of four fouled injectors: (a) spray images of the fouled injectors, (b) penetration lengths and standard deviations of the fouled injectors, and (c) a comparison of average spray structures and penetration lengths of the fouled and clean injectors.

3.3. Comparison of fouled and clean injectors by near-field spray analysis

A comparison of the near-field spray structure depending on the nozzle temperature and injection pressure is depicted in Fig. 5. In general, the atomization performance decreases as the fuel temperature and injection pressure decrease to lower values [17,18]. Moreover, deposits on the nozzle tip result in less interaction between the air and fuel near the nozzle holes [14]. The difference in the atomization performance between fouled and clean injectors was higher at lower injection pressures and lower fuel temperatures. Especially, large droplets were observed in the fouled injector under a nozzle temperature of 266 K and injection pressure of 100 bar, as shown in Fig. 5(a). However, as the injection pressure and nozzle temperature increased, it was hard to distinguish the difference between fouled and clean injectors with the naked eye in the near-field spray visualization. As shown in Fig. 4(a), the surface of the fouled injector tip was rough due to the deposits. Therefore, there was a high probability of causing cavitation and unstable fuel injection [19]. The spray boundary was superposed during injection to analyze the injection stability, as shown in Fig. 5(b). As the nozzle temperature and injection pressure decreased, the roughness of the spray boundary increased.

The atomization performance affects the emissions of the engine directly. At the end of injection, relatively large droplets that can cause the exhaust pollutants can exist near the nozzle tip. Therefore, comparisons of droplets at the end of injection were performed, as shown in Fig. 6(a). In near-field spray images, the residual droplets decreased as the nozzle temperature increased because of increasing evaporation and atomization performance. These results showed the same tendency regardless of the injectors. However, in the case of the clean injector, the residual droplets were clearly fewer in number compared to the fouled injector. There was more interaction between the air and fuel in the step-hole of the clean injector. In contrast, in the case of the fouled injector, the step-hole was fully clogged by deposits, so there was no breakup of droplets inside the step-hole because the air could not enter the step-hole. For these reasons, relatively long ligaments were observed near the injector tip in the fouled injector. The black pixels meaning droplets, except for those at the nozzle tip, were counted in the zoomed-in near-field spray images for quantitative analysis. Fig. 6(b) shows the number of black pixels of the zoomed-in near-field images. In all experimental conditions, the number of black pixels for the clean

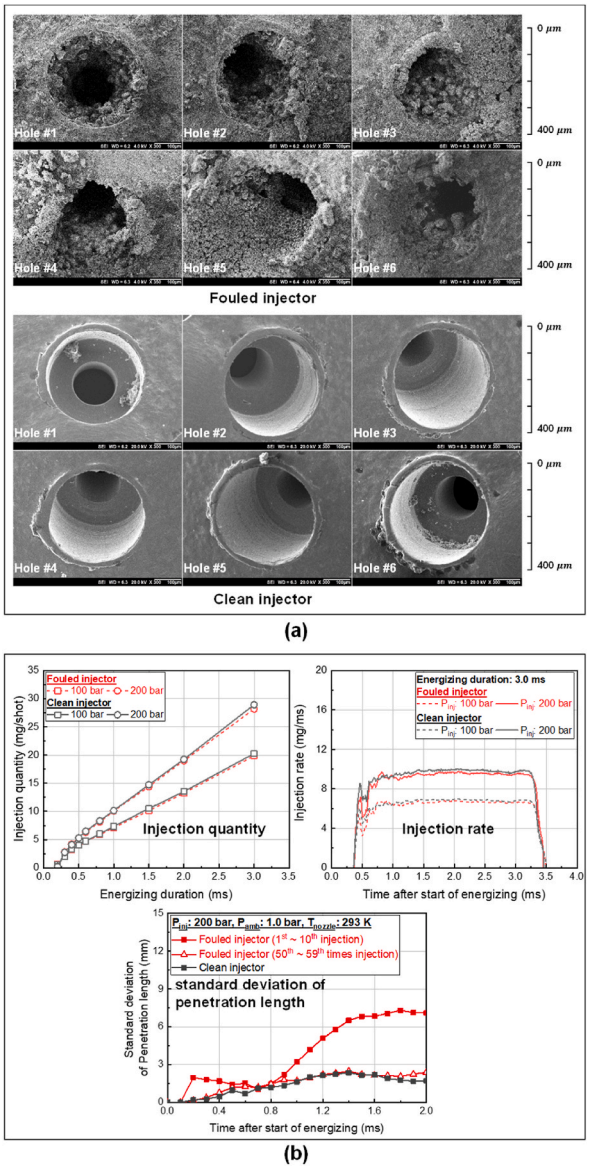

Fig. 4. Comparison of fouled and clean injectors: (a) SEM pictures of test injectors, and (b) injection quantity, injection rate, and standard deviation of penetration length.

injector was fewer than for the fouled injector because the atomization performance of the clean injector was high. Increasing the injection pressure resulted in fewer black pixels. Moreover, the number of black pixels decreased as the nozzle temperature increased regardless of the state of the injector. The number of black pixels was more affected by the injection conditions, such as the nozzle temperature and injection pressure, than the deposits. In the case of the high nozzle temperature condition, there was no dramatic difference in the number of black pixels between the fouled and clean injectors due to the rapid evaporation of fuel.

However, deposits can broadly affect the characteristics, such as the spray structure, penetration length, and spray angle. In a multi-hole injector, interaction between plumes plays an important role in the spray development process. The intensity of air entrainment varies depending on the intensity of interaction between plumes. Therefore, it is important to understand the intensity of interaction between plumes. The effects of deposits on the spray are depicted in Fig. 7. In general, the step-hole is used to increase the interaction between the fuel and air by forming a recirculation zone [20,21]. Air and fuel are mixed in the recirculation zone during the spray development, so that the atomization performance increases, as shown in Fig. 7(a) [22]. High atomization performance causes the dispersion of the spray resulting in a wide plume angle. However, the step-hole of the fouled injector was entirely clogged by deposits. Therefore, the intended role of the step-hole was frustrated. Deposits inside the step-hole acts as an extension of the orifice, limiting air recirculation and atomization, as shown in Fig. 7(b). Therefore, it induces a low exit turbulent kinetic energy of the deposit injector spray and reduces the atomization performance. The rough surface of the deposits also produces additional cavitation initiation inside

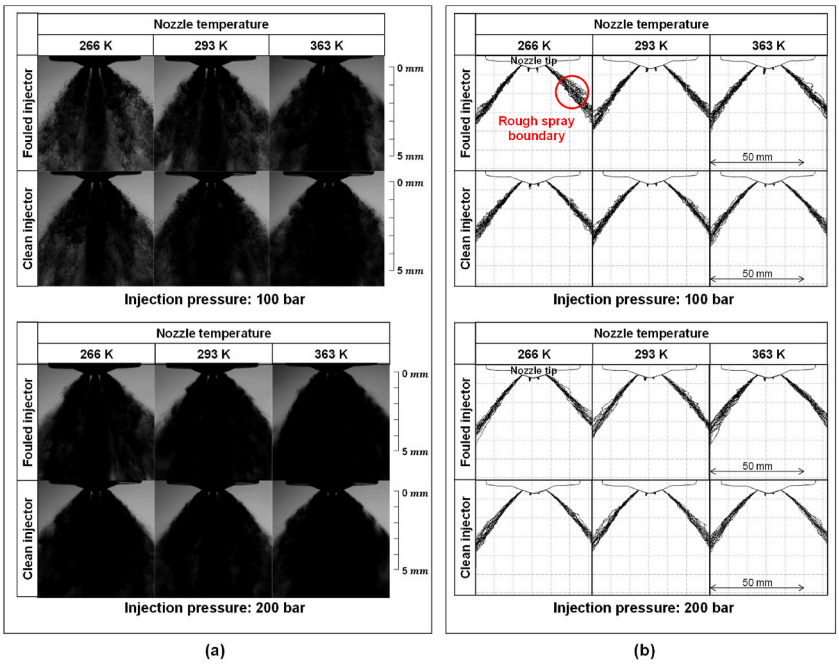

Fig. 5. Near-field spray images: (a) spray images in the middle of an injection (TASOE: 1.0 ms), and (b) superposed spray boundary images during fuel injection (TASOE: 0.4–2.1 ms).

the step-hole. Thus, cavitation with deposits reduces the effective flow area. Therefore, the mass flow is reduced. As a result, the fouled injector has a long spray penetration length and narrow plume angle compared to a clean injector due to its high exit velocity and low atomization performance.

When flash boiling occurs, bubbles are generated and grown in the liquid under superheated conditions. After the liquid is ejected from the nozzle, droplets are broken by an explosive power, as shown in Fig. 7(c). In this process, overlap between the plumes may occur as the plume angle increases. When the overlap between plumes occurs, the air entrainment rate and entrained air velocity increase during the spray development process, resulting in a large pressure drop [22]. The linked intensity between plumes affects the surrounding air that flows into the spray center. The inflow of surrounding air into the spray center is interrupted as plumes are strongly linked with each other. In this case, the clustered spray develops. When the spray clusters, spray characteristics, such as the spray structure, spray angle, and penetration length can be changed [23,24]. In general, as the flash boiling level increases, the linked intensity between plumes increases, and the spray collapse phenomenon that destroys the entire spray structure can be occurred. However, in the fouled injector, the plume angle is relatively small due to deposits. Therefore, the probability of an overlapped plume occurring decreases compared to the clean injector. However, it cannot be said that overlap between plumes occurs in all clean injectors. This is because the overlap between the plumes is affected by design factors, such as the distance between the nozzle holes and the spray targeting angle. Therefore, different linked intensity between plumes can be caused even under the same injection conditions depending on design factors. In conclusion, the deposit in the counter bore reduces the interaction intensity between plumes due to some reasons: restricted air and fuel mixing in the step-hole, reduced the effective flow area, and decreased atomization performance. Therefore, even when flash boiling occurs, the interaction intensity between the plumes is relatively small compared to a clean injector as shown in Fig. 7(d). The details about the entire spray structure revealed by far-field visualization under various injection conditions are depicted in the following Section 3.4.

3.4. Comparison of fouled and clean injectors by far-field spray analysis

In this section, far-field spray visualization was performed to compare the fouled and clean injectors under various injection conditions, such as ambient pressure, nozzle temperature, and flashing ratio.

3.4.1. Far-field spray characteristics depending on ambient pressure

The ambient pressure affects the plume-to-plume interaction intensity because the air quantity flowing into the spray center and drag force are affected by the ambient pressure [25,26]. Therefore, the spray characteristics of the fouled and clean injector were analyzed under various ambient pressures.

Fig. 8(a) shows the comparison of the spray structure depending on the ambient pressure in the fouled and clean injectors. The fouled injector had relatively low atomization performance because recirculation zone could not be formed in the step-hole. Therefore, it had a sharper spray structure compared to the clean injector. The difference of spray structure between the fouled and clean injector was also confirmed in the bottom-view results. Right images in Fig. 8(a) show the superposed spray. In the bottom-view, the spray of the fouled injector was sharper than that of the clean injector. In the fouled injector, each plume had a relatively sharp shape due to the

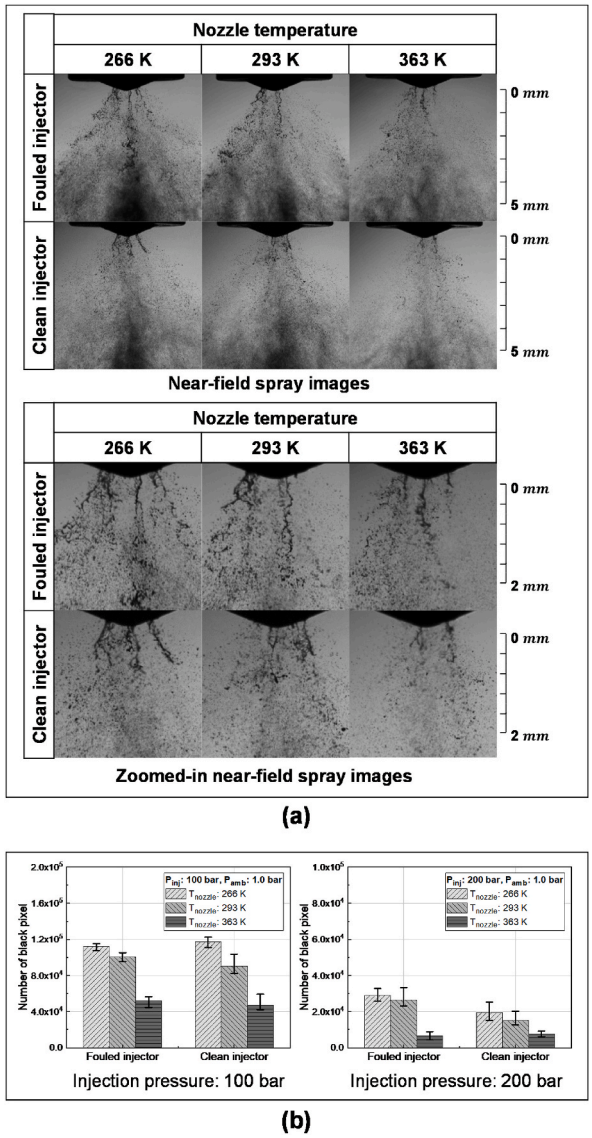

Fig. 6. Residual droplets at end of injection: (a) near-field spray images at end of injection (TASOE: 2.3 ms), and (b) the number of black pixels of a zoomed-in near-field image (TASOE: 2.3 ms).

low atomization performance and the decreases of effective flow area. The spray structure was quantitatively analyzed by calculating the spray angle, penetration length, and sharpness intensity, as shown in Fig. 8(b) and (c). The spray angles depending on ambient pressure in the fouled and clean injectors are shown in Fig. 8(b). In general, the spray angle is small when plumes cluster with each other due to a high plume-to-plume interaction [27]. A clean injector had a wider plume angle than the fouled injector because the dispersion of fuel increased. This is because atomization performance was improved by forming recirculation zone in the step-hole. A higher air entrainment rate occurred due to more interaction between plumes in a clean injector. Therefore, the spray angle was narrow due to the clustered spray in the clean injector. The difference of spray angle in the fouled and clean injectors increased when the ambient pressure increased. This is because as the ambient pressure increased, a higher air entrainment rate occurred due to an increase in the pressure difference. As a result, the plumes cluster rapidly into the spray center to recover the pressure drop [28,29]. However, there was no dramatic difference of penetration length between the fouled injector and the clean injector depending on the ambient pressure. This is because the spray collapse which can be caused by the high interaction between plumes did not occur. At an ambient pressure of 0.2 bar, the sharpness intensities of the fouled and clean injector were shown as a similar level of 0.15. This is because the effects of drag force on spray development were low. Therefore, the spray developed without a large disturbance by the surrounding air. On the other hand, when the ambient pressure increased, the sharpness intensity increased at the early stage of injection. And the sharpness intensities continuously decreased after TASOI of 0.2 ms in both test injectors. This is because the spray could not continuously develop and stagnated due to the drag force.

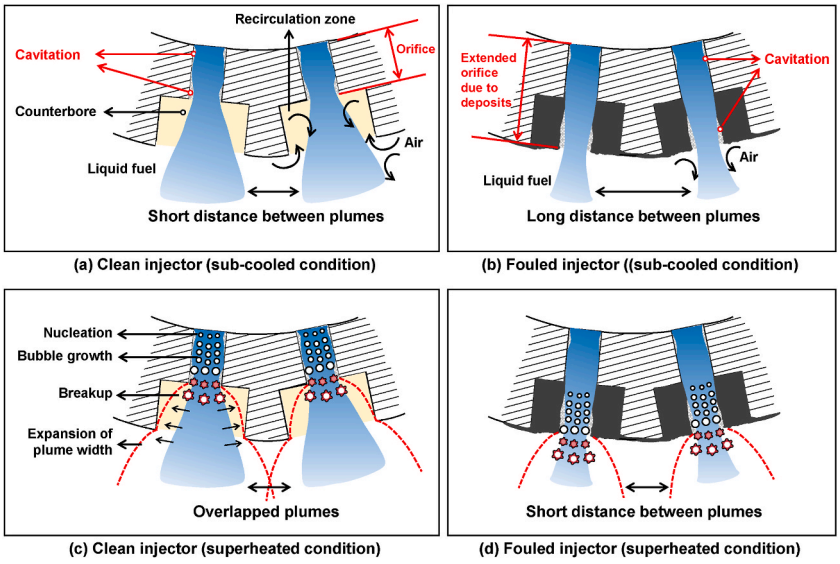

Fig. 7. A multi-hole comparison of the spray characteristics of clean and fouled injectors.

3.4.2. Far-field spray characteristics depending on the fuel temperature

Spray characteristics are affected by various physical properties, such as vapor pressure, density, surface tension, and viscosity [30,31]. These physical properties are directly influenced by the fuel temperature. Therefore, in this study, the spray visualization of fouled and clean injectors was performed under various fuel temperature conditions, from sub-zero temperatures to high fuel temperatures.

Fig. 9(a) shows the spray images depending on the fuel temperature in fouled and clean injectors. In the fouled injector, the step-hole was covered with deposits. Therefore, the air and fuel mixing did not occur in the recirculation area during the fuel injection. As a result, the atomization performance decreased. As the fuel temperature decreases, the atomization performance decreases due to the increase of the viscosity and surface tension of the fuel. However, when the fuel temperature decreased, there was no clear difference in the spray shape compared to room temperature in the clean injector. This is because the atomization was occurred sufficiently by the high injection pressure and the recirculation area in the step-hole. However, in the fouled injector, the atomization performance more decreased, so that the sharp spray structure was shown. Therefore, in the case of the low-temperature conditions, the difference in spray angle and penetration length between the fouled injector and the clean injector increased compared to room temperature.

On the other hand, when the fuel temperature increased, the atomization performance increased due to a decrease of the viscosity and surface tension of the fuel. Therefore, the plume angle increased. In the clean injector, the interaction between the plumes increased due to the increase of the plume angle, and the air entrainment rate increased compared to the fouled injector during the spray development process. Therefore, a pressure-drop at the center of the spray occurred, and the spray clustered in the axial direction. The spray collapse phenomenon occurs due to the high plume-to-plume interaction causing a clustered plume [32]. As a result, in the clean injector, the spray angle decreased and the penetration length increased compared to the fouled, as shown in Fig. 9(b) and (c).

3.4.3. Far-field spray characteristics depending on the flashing ratio

When flash boiling occurs, the spray structure changes due to the explosive force that is caused by a difference in the ambient and fuel vapor pressure [33,34]. In general, the spray structure gradually changes depending on the flashing ratio, which is called the superheated degree and is calculated by ambient pressure divided by vapor pressure [35,36]. Flash boiling is affected by various parameters, like the nozzle configuration and spray targeting angle of the plumes [37,38]. Especially, when the hole-to-hole distance is far, even though the plume angle increases due to flash boiling, the plume-to-plume interaction is relatively low. Therefore, different spray characteristics can be observed even under the same injection condition [39]. In this section, a macroscopic spray analysis depending on the flashing ratio in the fouled and clean injectors was conducted to understand the effects of flash boiling on the fouled injector.

Fig. 10(a) shows the spray images depending on the flashing ratio in the front and bottom-view. As the flashing ratio decreases, the difference between fuel vapor and ambient pressure increases, resulting in a large plume angle caused by a large explosive force [40]. Therefore, the probability of overlap between plumes increases. In the case of the fouled injector, the plume angle was smaller than that of the clean injector due to the deposits inside the step-hole. Therefore, the overlap intensity between plumes in the fouled injector was relatively low. This effect causing low interaction between plumes was reflected in the spray angle results, as shown in Fig. 10(b). The spray angle of the fouled injector was higher than that of the clean injector, even after flash boiling occurred. Fig. 10(c) shows the penetration length and sharpness intensity depending on the flashing ratio. Clustered plumes with high momentum developed after the spray collapse occurred at a TASOI of 1.2 ms in the clean injector. When the flashing ratio decreased to 0.77, the difference in the penetration length between the fouled and clean injector increased. The spray collapse occurred faster in the clean injector under a

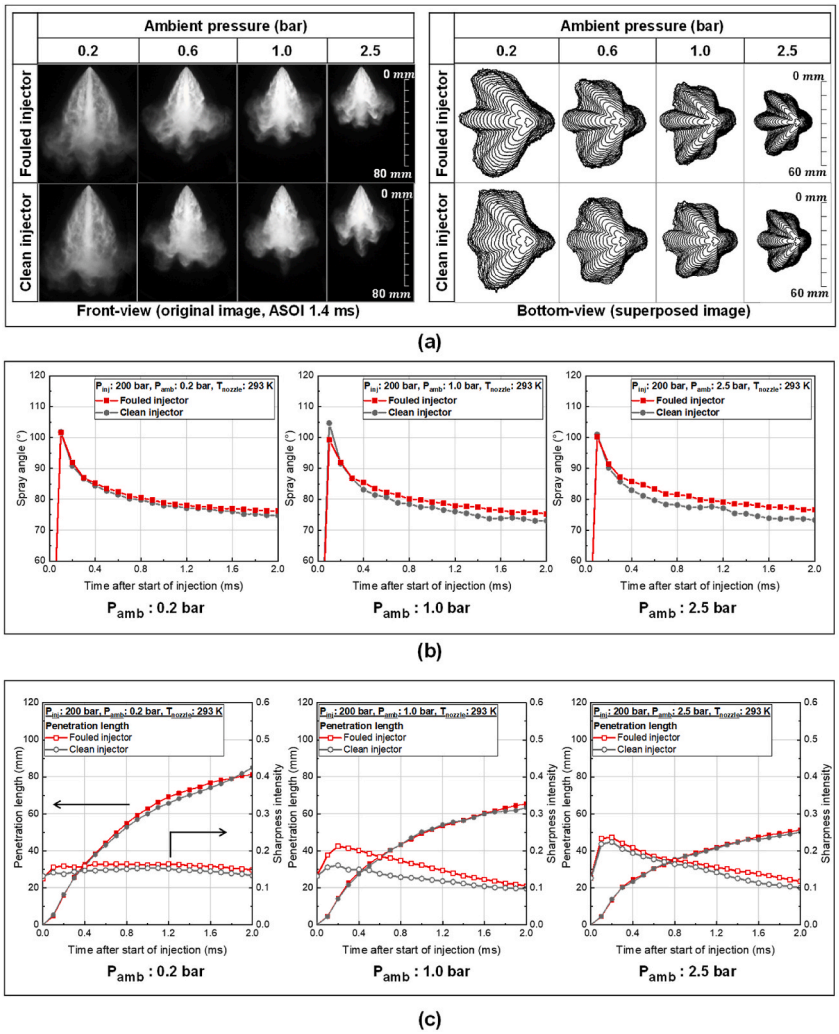

Fig. 8. Spray structure and quantitative indices results depending on ambient pressure: (a) spray structure, (b) spray angle, and (c) penetration length and sharpness intensity.

flashing ratio of 0.77 than under a flashing ratio of 1.28. Therefore, the penetration length increased compared to the flashing ratio of the 1.28 condition in both injectors. A previous study found that the spray structure totally collapses below a flashing ratio of 0.3 [41]. This region is called the flare flash region. In this region, the penetration length results were close to linear in both injectors. In conclusion, overlap between the plumes could occur even in a fouled injector when the flash boiling occurred. However, in the fouled injector, the overlap intensity between plumes was relatively low compared to the clean injector. Therefore, the pressure-drop at the spray center was lower than that of the clean injector. Moreover, the degree of spray clustering was relatively low. As a result, the increase of the momentum at the spray center by the spray collapse was larger in the clean injector. It caused a longer penetration length and narrower spray angle.

4. Conclusions

In this study, shot-to-shot variations of four fouled injectors and one clean injector were analyzed. The fouled injector, which had the greatest difference in spray characteristics from the clean injector, was selected as the representative fouled injector, and the spray characteristics depending on the injection conditions, such as the ambient pressure, fuel temperature, and flash boiling were investigated. Consequently, the following conclusions were drawn:

- The spray structure was different in the four fouled injectors because deposits was generated with different forms even under the same engine operating condition. In all fouled injectors, the spray structure was shown randomly depending on the injection order. In this study, the fouled injector with the greatest differences compared to the clean injector was selected as the representative fouled injector.

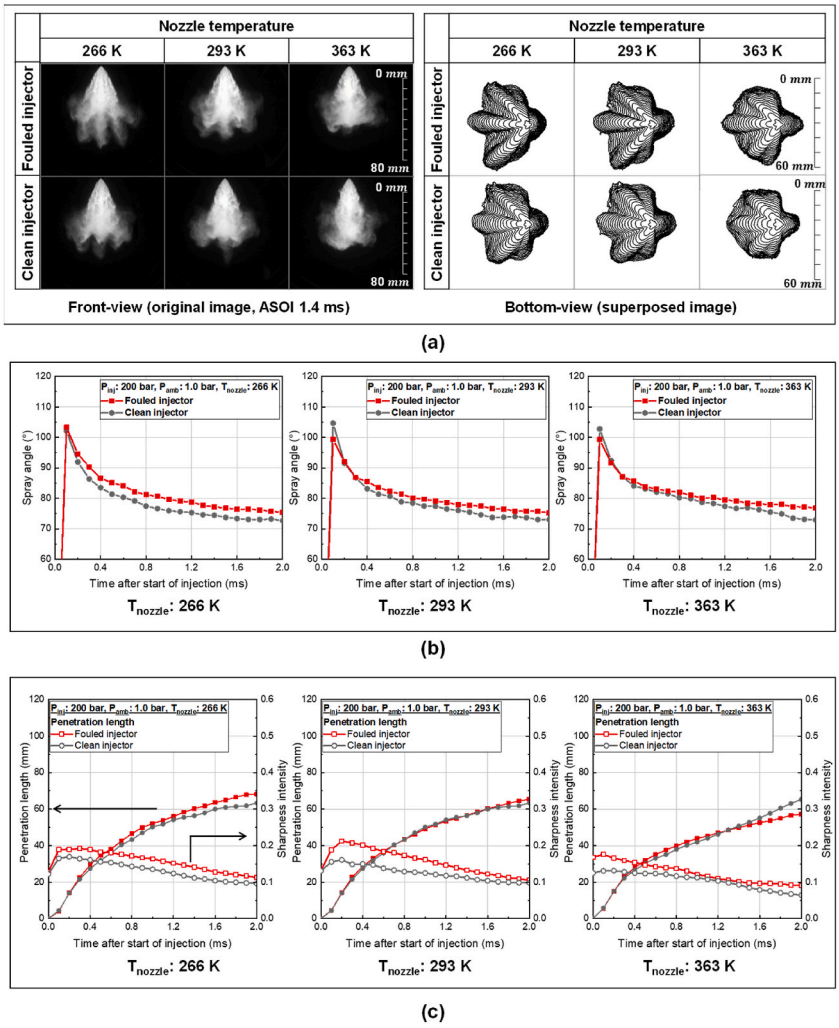

Fig. 9. Spray structure and quantitative indices results depending on fuel temperature: (a) spray structure, (b) spray angle, and (c) penetration length and sharpness intensity.

- There were relatively large droplets and long ligaments in the fouled injector compared to the clean injector due to the low atomization performance. Therefore, there were more residual droplets at the end of the injection around the nozzle tip in the fouled injector.
- The difference of spray angle in fouled and clean injectors was shown clearly as the ambient pressure increased. However, there was no clear difference of penetration length in both injectors regardless of the ambient pressure.
- In the sub-cooled condition, the fouled injector showed a wider spray angle than that of the clean injector, regardless of the fuel temperature. The penetration length between the two test injectors showed the greatest difference in the sub-zero temperature condition. In the high-temperature conditions, the spray collapse occurred at a TASOE of 1.2 ms only in the clean injector. The sharpness intensity showed a larger value in the fouled injector regardless of the temperature condition.
- Regardless of the flash boiling level, the fouled injector showed a wide spray angle. As the flashing ratio decreased, the interaction between the plumes increased, and the penetration length of the clean injector was larger than that of the fouled injector. The sharpness intensity showed a larger value in the fouled injector regardless of the occurrence of flash boiling.

Author contribution

Donghwan Kim: Writing- Original draft preparation, Investigation, Experiments.
Sungwook Park: Writing- Reviewing and Editing, Supervision.

Declaration of competing interest

The authors declare that they have no known competing financial interests or personal relationships that could have appeared to

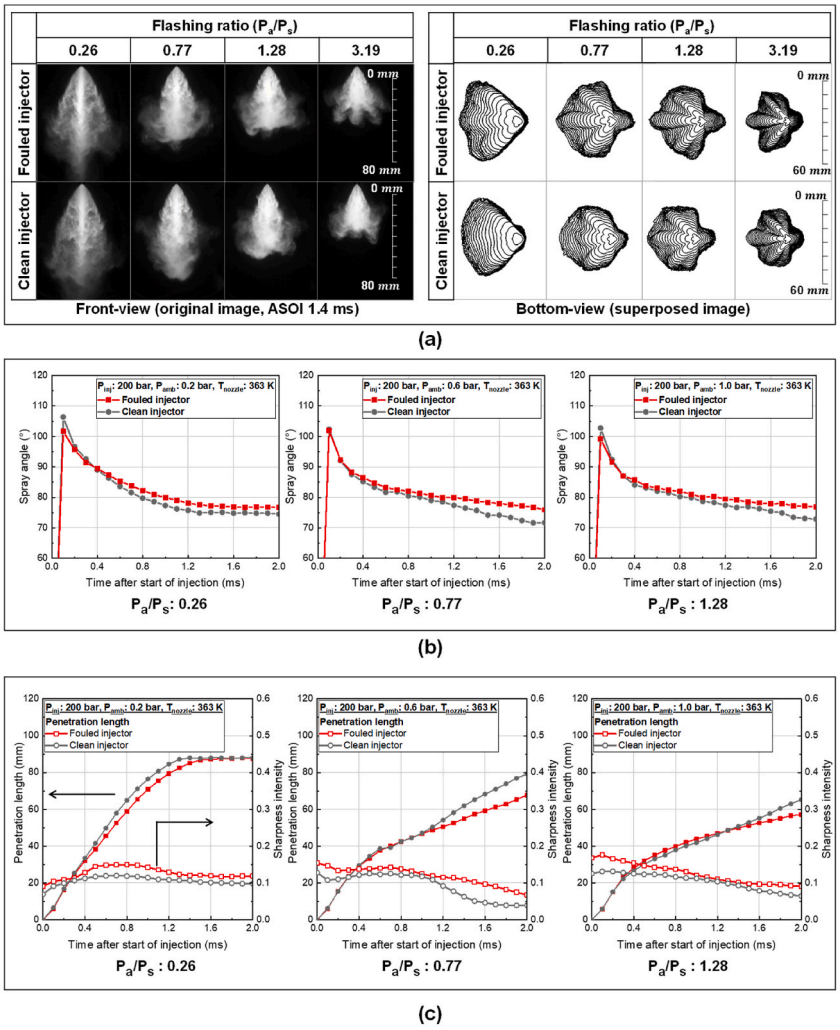

Fig. 10. Spray structure and quantitative indices results depending on flashing ratio: (a) spray structure, (b) spray angle, and (c) penetration length and sharpness intensity.

influence the work reported in this paper.

Data availability

No data was used for the research described in the article.

Acknowledgement

This work was supported by the Engine Advanced Development Team of the Hyundai Motor Group and the National Research Foundation of Korea(NRF) grant funded by the Korea government(MSIT). (2021R1A2C2011425).

References

[1] X. He, et al., Study of laminar combustion characteristics of gasoline surrogate fuel-hydrogen-air premixed flames, Int. J. Hydrogen Energy 44 (26) (2019) 13910–13922, https://doi.org/10.1016/j.ijhydene.2019.03.009.
[2] F. Liu, et al., Numerical study and cellular instability analysis of E30-air mixtures at elevated temperatures and pressures, Fuel 271 (2020), 117458, https://doi.org/10.1016/j.fuel.2020.117458.
[3] F. Zhao, M.-C. Lai, D.L. Harrington, Automotive spark-ignited direct-injection gasoline engines, Prog. Energy Combust. Sci. 25 (5) (1999) 437–562, https://doi.org/10.1016/S0360-1285(99)00004-0.
[4] J.B. Heywood, Internal Combustion Engine Fundamentals, McGraw-Hill Education, 2018.
[5] W. Du, et al., Effects of injection pressure on spray structure after wall impingement, Appl. Therm. Eng. 129 (2018) 1212–1218, https://doi.org/10.1016/j.applthermaleng.2017.10.083.
[6] Y. Bo, et al., A numerical investigation of injection pressure effects on wall-impinging ignition at low-temperatures for heavy-duty diesel engine, Appl. Therm. Eng. 184 (2021), 116366, https://doi.org/10.1016/j.applthermaleng.2020.116366.

[7] D. Kim, et al., Characteristics of in-cylinder flow and mixture formation in a high-pressure spray-guided gasoline direct-injection optically accessible engine using PIV measurements and CFD, Energy Convers. Manag. 248 (2021), 114819, https://doi.org/10.1016/j.enconman.2021.114819.
[8] P. Shayler, et al., Intake Port Fuel Transport and Emissions: the Influence of Injector Type and Fuel Composition, 1996, https://doi.org/10.4271/961996. SAE Technical Paper.
[9] A.A. Aradi, et al., Direct Injection Gasoline (DIG) Injector Deposit Control with Additives, 2003, https://doi.org/10.4271/2003-01-2024. SAE Technical Paper.
[10] H. Sandquist, et al., Influence of fuel parameters on deposit formation and emissions in a direct injection stratified charge SI engine, SAE Trans. (2001) 1537–1548. https://www.jstor.org/stable/44742754.
[11] H. Xu, et al., Fuel injector deposits in direct-injection spark-ignition engines, Prog. Energy Combust. Sci. 50 (2015) 63–80, https://doi.org/10.1016/j.pecs.2015.02.002.
[12] Z. Zhang, et al., Effects of GDI injector deposits on spray and combustion characteristics under different injection conditions, Fuel 278 (2020), 118094, https://doi.org/10.1016/j.apenergy.2020.114538.
[13] B. Wang, et al., Investigation of deposit effect on multi-hole injector spray characteristics and air/fuel mixing process, Fuel 191 (2017) 10–24, https://doi.org/10.1016/j.fuel.2016.11.055.
[14] J. Zhou, et al., Characteristics of near-nozzle spray development from a fouled GDI injector, Fuel 219 (2018) 17–29, https://doi.org/10.1016/j.fuel.2018.01.070.
[15] H. Song, et al., The effects of surface temperature on the deposit behaviors of gasoline on a hot surface, Fuel 215 (2018) 111–122, https://doi.org/10.1016/j.fuel.2017.11.017.
[16] J.N. Stenzler, et al., Penetration of liquid jets in a cross-flow, Atomization Sprays 16 (8) (2006), https://doi.org/10.1615/AtomizSpr.v16.i8.30.
[17] X. Wang, A. Lefebvre, Influence of fuel temperature on atomization performance of pressure-swirl atomizers, J. Propul. Power 4 (3) (1988) 222–227, https://doi.org/10.2514/3.23052.
[18] J. Jia, et al., Spray atomization characteristics of biomass pyrolysis tar: influence of methanol addition, temperature, and atomization pressure, Energy 242 (2022), 122534, https://doi.org/10.1016/j.energy.2021.122534.
[19] B. Wang, et al., Numerical investigation of the deposit effect on GDI injector nozzle flow, Energy Proc. 105 (2017) 1671–1676, https://doi.org/10.1016/j.egypro.2017.03.545.
[20] R. Payri, et al., Analysis of counterbore effect in five diesel common rail injectors, Exp. Therm. Fluid Sci. 107 (2019) 69–78, https://doi.org/10.1177/1468087418819250.
[21] R. Payri, et al., Impact of counter-bore nozzle on the combustion process and exhaust emissions for light-duty diesel engine application, Int. J. Engine Res. 20 (1) (2019) 46–57, https://doi.org/10.1177/1468087418819250.
[22] B. Wang, et al., Numerical analysis of deposit effect on nozzle flow and spray characteristics of GDI injectors, Appl. Energy 204 (2017) 1215–1224.
[23] P. Sphicas, et al., Inter-plume aerodynamics for gasoline spray collapse, Int. J. Engine Res. 19 (10) (2018) 1048–1067, https://doi.org/10.1177/1468087417740306.
[24] H. Guo, et al., Radial expansion of flash boiling jet and its relationship with spray collapse in gasoline direct injection engine, Appl. Therm. Eng. 146 (2019) 515–525, https://doi.org/10.1016/j.applthermaleng.2018.10.031.
[25] I. Roisman, L. Araneo, C. Tropea, Effect of ambient pressure on penetration of a diesel spray, Int. J. Multiphas. Flow 33 (8) (2007) 904–920, https://doi.org/10.1016/j.ijmultiphaseflow.2007.01.004.
[26] J.-H. Park, et al., Effect of injection conditions on the spray behaviors of the multi-hole GDI injector, Transactions of the Korean Society of Automotive Engineers 20 (2) (2012) 116–122, https://doi.org/10.7467/KSAE.2012.20.2.116.
[27] D. Kim, S. Park, Effects of nozzle hole configuration of a multi-hole type gasoline direct injector on spray development under flash boiling conditions, Int. J. Engine Res. 22 (9) (2021) 2997–3012, https://doi.org/10.1177/1468087420960026.
[28] L. Du, K.J. Folliard, Mechanisms of air entrainment in concrete, Cement Concr. Res. 35 (8) (2005) 1463–1471, https://doi.org/10.1016/j.cemconres.2004.07.026.
[29] Q. Xu, et al., Investigation of two-hole flash-boiling plume-to-plume interaction and its impact on spray collapse, Int. J. Heat Mass Tran. 138 (2019) 608–619, https://doi.org/10.1016/j.ijheatmasstransfer.2019.04.111.
[30] Z. Van Romunde, et al., Effect of fuel properties on spray development from a multi-hole DISI engine injector, SAE Trans. (2007) 1313–1331. https://www.jstor.org/stable/44699359.
[31] T.J. Callahan, et al., Effects of Fuel Properties on Diesel Spray Characteristics, Southwest Research Institute, San Antonio, TX, 1987.
[32] Y. Li, et al., An exploration on collapse mechanism of multi-jet flash-boiling sprays, Appl. Therm. Eng. 134 (2018) 20–28, https://doi.org/10.1016/j.applthermaleng.2018.01.102.
[33] E. Sher, T. Bar-Kohany, A. Rashkovan, Flash-boiling atomization, Prog. Energy Combust. Sci. 34 (4) (2008) 417–439, https://doi.org/10.1016/j.pecs.2007.05.001.
[34] Z. Zhang, et al., Characteristics of trans-critical propane spray discharged from multi-hole GDI injector, Exp. Therm. Fluid Sci. 99 (2018) 446–457, https://doi.org/10.1016/j.expthermflusci.2018.07.025.
[35] J. Lacey, et al., Generalizing the behavior of flash-boiling, plume interaction and spray collapse for multi-hole, direct injection, Fuel 200 (2017) 345–356, https://doi.org/10.1016/j.fuel.2017.03.057.
[36] S. Li, Y. Zhang, W. Qi, Quantitative study on the influence of bubble explosion on evaporation characteristics of flash boiling spray using UV-LAS technique, Exp. Therm. Fluid Sci. 98 (2018) 472–479, https://doi.org/10.1016/j.expthermflusci.2018.03.025.
[37] S. Yang, et al., Characteristics and correlation of nozzle internal flow and jet breakup under flash boiling conditions, Int. J. Heat Mass Tran. 127 (2018) 959–969, https://doi.org/10.1016/j.ijheatmasstransfer.2018.07.109.
[38] X. Zhang, et al., Effect of fuel temperature on cavitation flow inside vertical multi-hole nozzles and spray characteristics with different nozzle geometries, Exp. Therm. Fluid Sci. 91 (2018) 374–387, https://doi.org/10.1016/j.expthermflusci.2017.06.006.
[39] M. Chang, S. Park, Spray characteristics of direct injection injectors with different nozzle configurations under flash-boiling conditions, Int. J. Heat Mass Tran. 159 (2020), 120104, https://doi.org/10.1016/j.ijheatmasstransfer.2020.120104.
[40] C. Ji, et al., Experimental investigation on high-pressure high-temperature spray flash evaporation and the characteristic Jakob number, Exp. Therm. Fluid Sci. 102 (2019) 94–100, https://doi.org/10.1016/j.expthermflusci.2018.10.018.
[41] A. Wood, G. Wigley, J. Helie, Flash boiling sprays produced by a 6-hole GDI injector, in: 17th International Symposium on Applications of Laser Techniques to Fluid Mechanics, 2014. Lisbon, Portugal.

Nomenclature

P_{amb}: Ambient pressure
P_{intake}: Intake pressure
T_{nozzle}: Nozzle tip temperature

Abbreviations

ASOI: After Start of Injection
CVC: Constant Volume Chamber
DBI: Diffuse Back-illumination
GDI: Gasoline Direct Injection

PFI: Port Fuel Injection
SEM: Scanning Electron Microscope
TASOE: Time After Start of Energizing